Reply*

MARTIN VISBECK

Lamont-Doherty Earth Observatory, and Department of Earth and Environmental Sciences, Columbia University, Palisades, New York

ALEX HALL

Department of Atmospheric Sciences, University of California, Los Angeles, Los Angeles, California

6 August 2003 and 24 October 2003

Climate variability in the Southern Hemisphere is receiving increasing attention due to both the large greenhouse gas–forced response that many climate models exhibit in polar regions (Houghton et al. 2001), and observed recent trends in the southern annular mode (SAM) index (Thompson and Solomon 2002; Thompson et al. 2000). Hall and Visbeck (2002) described regional impacts of the SAM in a coarse-resolution coupled climate model. The overwhelming dominance of this mode in the interannual-to-interdecadal variability of the model's atmosphere and ocean led us to the hypothesis that most of the interannual climate variability of the real world would also be associated with the SAM. This statement was contested in a recent commentary by White (2003), who claims that the Antarctic circumpolar wave (ACW) is the dominant mode of interannual climate variability in the Southern Hemisphere. He presented supporting evidence from an analysis of the sea level pressure anomaly data obtained from the National Centers for Environmental Prediction–National Center for Atmospheric Research (NCEP–NCAR) atmospheric reanalysis.

Modes of Southern Hemisphere atmospheric variability are often identified in terms of the first few empirical orthogonal functions (EOFs) of pressure or geopotential height data (Kidson 1988, 1999; Mo 2000; Renwick 2002). Most studies have used 500-hPa height anomalies, with fewer studies using pressure levels closer to the surface (850 hPa). However, the choice of level makes little difference, due to the equivalent barotropic nature of month-to-month atmospheric variability (e.g., Thompson and Wallace 2000). Mo (2000) computed the first three EOF patterns of 500-hPa height data and discussed the principal component time series for the whole lengths of the NCEP–NCAR reanalysis period (1949–98). White (2003), however, restricted his analysis to the period between 1982 and 2001, perhaps because he doubts the accuracy of the first 20 yr of NCEP data. To facilitate direct comparison to White's results, we computed EOFs of the area-weighted monthly height anomalies of the 850-hPa pressure surface for nearly the same time period (1980–2002). However, we employ a standard rather than complex EOF analysis technique. Complex EOF analysis is often used to identify propagating anomalies (arising, e.g., from coupled ocean–atmosphere interactions). It typically combines two standard EOF modes into one complex mode. There is, therefore, a direct correspondence between our standard EOF patterns and White's complex EOF patterns, as we discuss below.

Figures 1a–1c shows the first three standard EOF patterns normalized to unit spatial variance. In agreement with most previous studies, we find that the SAM is represented by the first EOF and accounts for ~20% of the total variance followed by two modes, which each account for ~10% of the variance. The second and third modes both show maximum amplitude in the Pacific and have often been associated with a propagating wave train within the Pacific–South American (PSA) sector. They have been referred to as the PSA teleconnection pattern (Ghil and Mo 1991; Karoly 1989; Kiladis and Mo 1998; Kidson 1999; Yuan and Martinson 2000). We refer to them as PSA-1 and PSA-2.

All of the power of White's (2003) first complex EOF is contained in the 180° phase, which closely resembles our SAM pattern. Our SAM principal component time

* Lamont-Doherty Earth Observatory Contribution Number 6532.

Corresponding author address: Dr. Martin Visbeck, Lamont-Doherty Earth Observatory, and Dept. of Earth and Environmental Sciences, Columbia University, Oceanography Building, Room 204C, RT 9W, Palisades, NY 10964-8000.
E-mail: visbeck@ldeo.columbia.edu

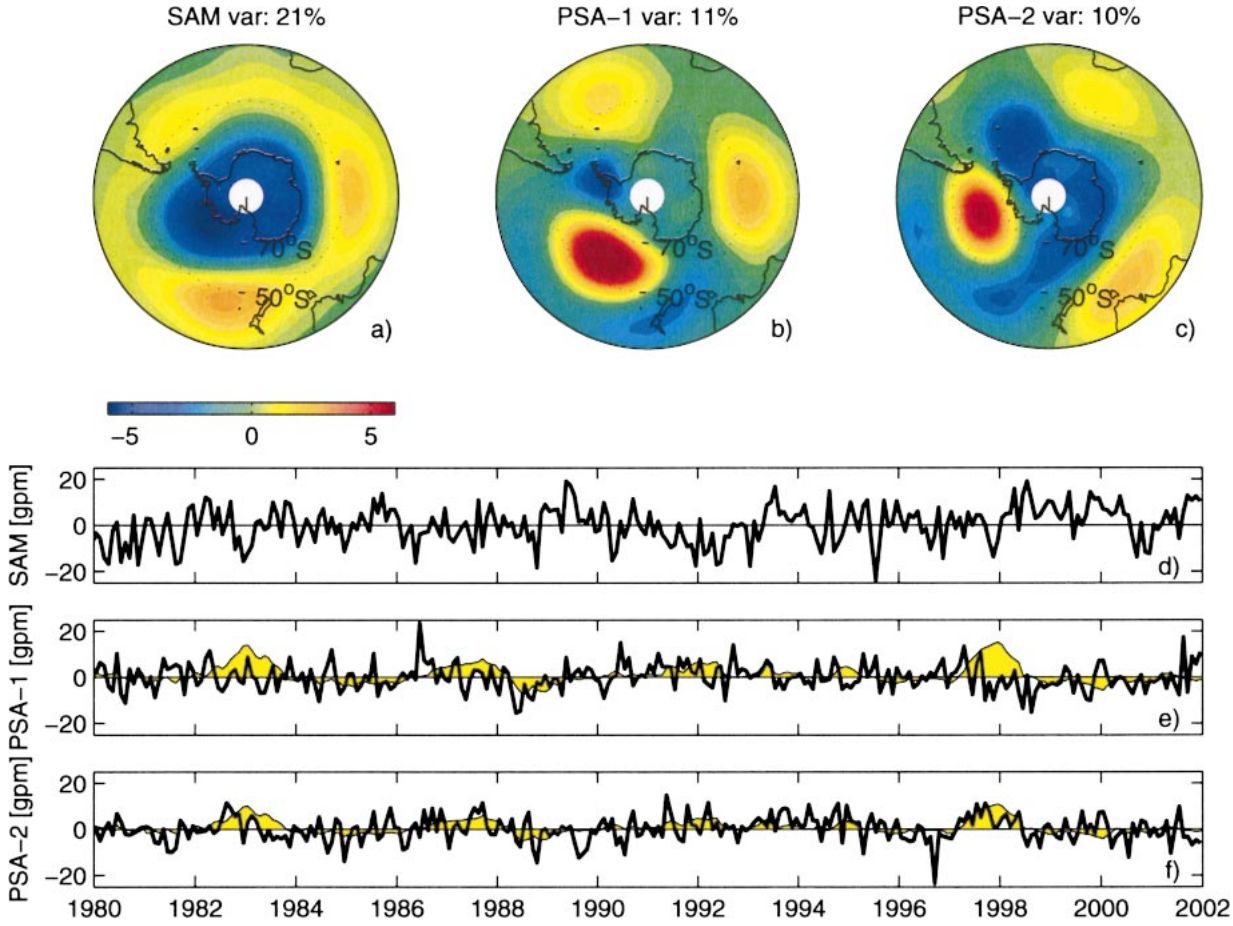

FIG. 1. (a)–(c) The first three EOF modes of monthly area-weighted 850-hPa pressure surface height anomalies. The data were reduced by sampling every third point in the zonal direction (7.5°) between 82° and 30°S and then normalized by cosine of latitude, prior to the decomposition, in order to ensure a equal area representation. The cosine latitude factor was multiplied back to the pattern prior to display. (d)–(f) The principal component of the three EOFs (SAM, PSA-1, and PSA-2, respectively) are given in geopotential meters. The principal component time series PSA-1 and PSA-2 are shown together with scaled Niño-3 SST anomalies (yellow) for reference to ENSO.

series (Fig. 1d) is also very similar both to White's and that of Gong and Wang (1999). We use the standard SAM definition, where a positive index indicates a stronger-than-normal pressure gradient between the subpolar low and subtropical high regions (Thompson and Wallace 2000). However, White has chosen a phase reference, which resulted in a negative polarity, compared to this definition, so that his SAM time series appears anticorrelated to ours.

Our PSA-1 and PSA-2 patterns correspond to White's second complex EOF at the 180° and 270° phase, respectively. Both modes show a weak relationship with ENSO (Figs. 1e–f). The monthly (annual June–May season) zero-lag correlation between the PSA-1 index and sea surface temperature anomalies in the Niño-3 region (5°N–5°S, 150°–90°W) is 0.2 (0.5), and slightly higher for the PSA-2 index with 0.3 (0.6). White refers to the combined, possibly propagating, PSA pattern as the ACW. Visual inspection suggests that his ACW time series is close to our PSA-1 (EOF-2) principal component with opposite polarity. However, one cannot be sure because he used a phase demodulation technique to obtain a real time series from the complex principal component time sequence, which was not fully explained.

The power spectra of the three time series (Fig. 2) was computed based on four 5.3-yr-long overlapping segments and shows spectral shapes that are consistent with an autoregressive red noise process. The dotted lines are the maximum and minimum values from a large number of randomly generated time series of the same length, energy, and lag-1 persistence as the SAM time series. In contrast to White's (2003) results, our spectral analysis shows that the SAM dominates the PSA variance for almost all frequencies. In particular, we find no significant reduction in SAM energy for low frequencies. The difference between the SAM and PSA spectra is only barely significant for any particular spectral band, which should not be surprising, given the shortness of the time series. However, because the SAM

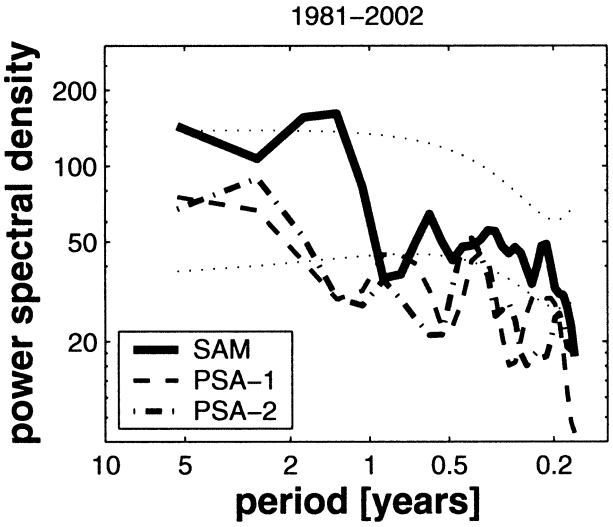

FIG. 2. Spectral estimates based on four 5.3-yr-long segments of the SAM, PSA-1, and PSA-2 principal components. The dotted lines are the envelope of spectral estimates based on a large number of random times series with the same energy and length as the SAM time series and a lag-1 autocorrelation of 0.25. The lag-1 autocorrelation of the SAM and PSA time series varied between 0.15 and 0.3. Thus, the dotted lines are also a reasonable estimate for the uncertainty in the PSA spectra, but would have to be vertically shifted to match the mean energy level of the PSA spectra.

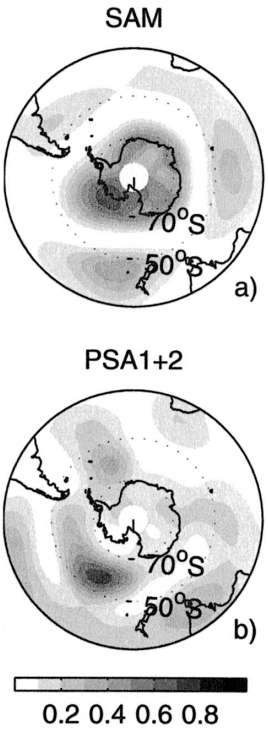

FIG. 3. Fraction of local monthly 850-hPa height variance between 1980 and 2002 associated with the (a) SAM and (b) combined PSA-1 and PSA-2 modes.

energy is consistently larger by a factor of 2 than both of the PSA modes, it is very unlikely that the overall dominance of the SAM will diminish once longer reliable time series are available. This result calls into question most of the summary statements made by White that might have been based on a peculiarity in his spectral estimate.

Finally, we compute the monthly variance associated with the SAM (see also Gong and Wang 1999) and that of the combined PSA-1 and PSA-2 modes (Figs. 3a and 3b). Both modes contribute significantly to the variability of the 850-hPa pressure surface in different parts of the Southern Hemisphere. SAM seems to dominate the pressure changes in the vicinity of the Antarctic continent and, thus, is largely influencing the strength of the circumpolar winds, as suggested in Hall and Visbeck (2002). The combined PSA modes, however, contribute mostly to pressure changes in the Pacific sector between 50° and 65°S and, thus, can influence the departures from the zonal atmospheric circulation. For example, the PSA-2 mode has been associated with an ENSO-forced dipolar surface air temperature and sea ice response between the Atlantic and Pacific sectors (Yuan and Martinson 2000).

On the basis of our diagnostic of the NCEP–NCAR reanalysis data, we maintain that the SAM is the dominant mode of atmospheric pressure variability on all time scales, at least out to 5 yr. Neither White nor we have presented any new evidence for the respective impacts that the SAM or PSA might have on observed interannual variability of the ocean circulation or properties. Thus, we see no reason to depart from our working hypothesis as presented in Hall and Visbeck (2002) that changes in the circumpolar zonal winds, associated with the SAM, will dominate the interannual ocean variability.

Acknowledgments. Funding for this work was obtained by a grant from the National Science Foundation ATM00-02833. The paper has benefitted from discussion with Yochanan Kushnir and Xiaojun Yuan.

REFERENCES

Ghil, M., and K. Mo, 1991: Intraseasonal oscillations in the global atmosphere. Part II: Southern Hemishpere. *J. Atmos. Sci.,* **48,** 780–792.

Gong, D., and S. Wang, 1999: Definition of Antarctic Oscillation index. *Geophys. Res. Lett.,* **26,** 459–462.

Hall, A., and M. Visbeck, 2002: Synchronous variability in the Southern Hemisphere atmosphere, sea ice, and ocean resulting from the annular mode. *J. Climate,* **15,** 3043–3057.

Houghton, J. T., Y. Ding, D. J. Griggs, M. Noguer, P. van der Linden, X. Dai, and K. Maskell, Eds., 2001: *The Third Assessment Report of the Intergovernmental Panel on Climate Change (IPCC).* Cambridge University Press, 944 pp.

Karoly, D. J., 1989: Southern Hemisphere circulation features associated with El Niño–Southern Oscillation events. *J. Climate,* **2,** 1239–1252.

Kidson, J. W., 1988: Indices of the Southern Hemisphere zonal wind. *J. Climate,* **1,** 183–194.

——, 1999: Principal modes of Southern Hemisphere low-frequency

variability obtained from NCEP–NCAR reanalyses. *J. Climate,* **12,** 2808–2830.

Kiladis, G. N., and K. C. Mo, 1998: Interannual and intraseasonal variability in the Southern Hemisphere. *Meteorology of the Southern Hemisphere, Meteor. Monogr.,* No. 49, Amer. Meteor. Soc., 307–337.

Mo, K. C., 2000: Relationships between low-frequency variability in the Southern Hemisphere and sea surface temperature anomalies. *J. Climate,* **13,** 3599–3610.

Renwick, J. A., 2002: Southern Hemisphere circulation and relations with sea ice and sea surface temperature. *J. Climate,* **15,** 3058–3068.

Thompson, D. W. J., and J. M. Wallace, 2000: Annular modes in the extratropical circulation. Part I: Month-to-month variability. *J. Climate,* **13,** 1000–1016.

——, and S. Solomon, 2002: Interpretation of recent Southern Hemisphere climate change. *Science,* **296,** 895–899.

——, J. M. Wallace, and G. C. Hegerl, 2000: Annular modes in the extratropical circulation. Part II: Trends. *J. Climate,* **13,** 1018–1036.

White, W. B., 2003: Comment on ''Synchronous Variability in the Southern Hemisphere atmosphere, sea ice, and ocean resulting from the annular mode.'' *J. Climate,* **17,** 2249–2254.

Yuan, X. J., and D. G. Martinson, 2000: Antarctic sea ice extent variability and its global connectivity. *J. Climate,* **13,** 1697–1717.